

## Atomic force microscope investigation of the boundary-lubricant layer in articular cartilage

S.M.T. Chan <sup>†\*</sup>, C.P. Neu <sup>†‡</sup>, G. DuRaine <sup>†</sup>, K. Komvopoulos <sup>§</sup>, A.H. Reddi <sup>†</sup>

<sup>†</sup>Center for Tissue Regeneration and Repair, Department of Orthopaedic Surgery, University of California, Davis, Medical Center, Sacramento, CA 95817, USA

<sup>‡</sup>Weldon School of Biomedical Engineering, Purdue University, West Lafayette, IN 47907, USA

<sup>§</sup>Department of Mechanical Engineering, University of California, Berkeley, CA 94720, USA

### ARTICLE INFO

#### Article history:

Received 29 September 2009

Accepted 26 March 2010

#### Keywords:

Articular cartilage

Boundary lubrication

Enzymes

Friction coefficient

Lubricin

Superficial zone protein (SZP)

### SUMMARY

**Objective:** To determine the roles of superficial zone protein (SZP), hyaluronan (HA), and surface-active phospholipids (SAPL) in boundary lubrication of articular cartilage through systematic enzyme digestion using trypsin, hyaluronidase, and phospholipase-C (PLC) surface treatments.

**Methods:** The friction coefficient of articular cartilage surfaces was measured with an atomic force microscope (AFM) before and after enzyme digestion. Surface roughness, adhesion, and stiffness of the articular surface were also measured to determine the mechanism of friction in the boundary lubrication regime. Histology and transmission electron microscopy were used to visualize the surface changes of treatment groups that showed significant friction changes after enzyme digestion.

**Results:** A significant increase in the friction coefficient of both load-bearing and non load-bearing regions of the joint was observed after proteolysis by trypsin. Treatment with trypsin, hyaluronidase, or PLC did not affect the surface roughness. However, trypsin treatment decreased the adhesion significantly. Results indicate that the protein component at the articular cartilage surface is the main boundary lubricant, with SZP being a primary candidate. The prevailing nanoscale deformation processes are likely plastic and/or viscoelastic in nature, suggesting that plowing is the dominant friction mechanism.

**Conclusions:** The findings of this study indicate that SZP plays an intrinsic and critical role in boundary lubrication at the articular surface of cartilage, whereas the effects of HA and SAPL on the tribological behavior are marginal.

© 2010 Osteoarthritis Research Society International. Published by Elsevier Ltd. All rights reserved.

### Introduction

Articular cartilage is essential for load bearing and lubrication in synovial joints. Normal joint articulation is maintained by mixed modes of lubrication, including hydrodynamic and boundary lubrication at the extremes. The thickness of the hydrodynamic film depends on the fluid viscosity, contact load, and relative velocity of the surfaces. Boundary lubrication dominates under conditions of reduced fluid viscosity, low relative velocity, and/or increased contact load. Because boundary-lubricated surfaces are separated by a lubricant film of thickness less than the effective surface roughness, contact between surface asperities is unavoidable. Prevention of cartilage wear greatly depends on the presence of

a conformal boundary film that reduces the shear strength at asperity contact interfaces. Although hydrodynamic lubrication is essential for low friction in the hydrated cartilage tissue<sup>1,2</sup>, the lack of an effective boundary lubricant that protects the tissue when joint movement conditions do not favor the formation of a hydrodynamic film can lead to precocious joint degeneration<sup>3,4</sup>.

Several molecules have been proposed as the key boundary lubricant of articular cartilage, including superficial zone protein (SZP), hyaluronan (HA), and surface-active phospholipids (SAPL). SZP, also known as lubricin and PRG4, is expressed by cells in the superficial zone and synovium and localizes at the cartilage surface. It contains an extensive mucin-like region substituted by O-linked oligosaccharides<sup>3,5</sup>, which reduce friction through the development of repulsive forces<sup>3,5</sup>. HA is a glycosaminoglycan (GAG), which is a major component of synovial fluid, imparting the fluid viscosity and elasticity needed to transfer loads across the cartilage–cartilage interface<sup>6,7</sup>. Although HA is critical for hydrodynamic lubrication<sup>2</sup> and may provide boundary lubrication in synovial fluid<sup>8</sup>, its intrinsic lubricating efficacy in cartilage has not been

\* Address correspondence and reprint requests to: Stephanie Chan, Center for Tissue Regeneration and Repair, Department of Orthopaedic Surgery, University of California, Davis, Medical Center, Research Building 1, Room 2000, 4635 Second Avenue, Sacramento, CA 95817, USA. Tel: 1-916-734-5757; Fax: 1-916-734-5750.

E-mail address: [smtchan@ucdavis.edu](mailto:smtchan@ucdavis.edu) (S.M.T. Chan).

demonstrated. SAPL is an endogenous component of synovial fluid<sup>9</sup> that may act as a hydrophobic surfactant adsorbed onto the articular surface providing the contact angle and wettability observed in previous studies<sup>2,9</sup>.

Articular cartilage friction at the nanoscale may be measured using an atomic force microscope (AFM). Even nominally smooth surfaces, such as articular cartilage, exhibit frictional resistance during articulation with other surfaces, resulting from localized solid–solid interactions at the asperity scale. AFM is particularly suited for friction measurements in the boundary lubrication regime because it can simulate interactions at single asperity contacts under high contact pressures<sup>10,11</sup>. Nanoscale friction behavior depends on the sliding dynamics of interacting asperities and properties of the surface (boundary) layer<sup>12</sup>. Characterizing the surface roughness, contact forces, and mechanical properties of the boundary layer is critical to understanding the friction mechanisms at the tissue surface.

Previous studies have investigated the effects of enzymatic digestion on the putative boundary lubricants of tendon<sup>13</sup>, synovial fluid<sup>14,15</sup>, and synovial fluid co-incubated with full-thickness articular cartilage<sup>16</sup>. Although the latter study minimized fluid effects on lubrication by providing an equilibration preload time to depressurize the tissue, the results cannot be interpreted in the context of articular cartilage boundary lubrication for the following reasons. First, as noted by others<sup>14</sup>, the phospholipase A<sub>2</sub> used to digest SAPL contained proteolytic activity. Second, full-thickness patellar articular cartilage co-incubated with synovial fluid during enzymatic digestion confounded the effects of both the synovial fluid lubricating activity and the digestion of extracellular matrix protein, HA, and phospholipids.

The objective of this study was to elucidate the roles of SZP, HA, and SAPL in articular cartilage boundary lubrication. Friction coefficient and surface roughness measurements, and topography images obtained with an AFM before and after surface enzymatic digestion of SZP, HA, or SAPL were used to examine the roles of candidate molecules in boundary lubrication. Additionally, stiffness, adhesion, transmission electron microscopy, and histology data were used to analyze the dominant friction mechanism. Enzyme treatment of the primary boundary lubricant was hypothesized to increase the friction coefficient and roughness of the articular surface.

## Materials and methods

### Materials

Dulbecco's Modified Eagle's Medium (DMEM)/F12 and antibiotics were purchased from Invitrogen (Carlsbad, CA). Trypsin (15400-054, Invitrogen) was diluted to 0.5%<sup>13,17</sup>, hyaluronidase (LS005475, Worthington, Lakewood, NJ) was diluted to 0.1% (7500 units/mL)<sup>13,18</sup>, and phospholipase C (PLC) (P7633, Sigma–Aldrich, St. Louis, MO) was diluted to 0.44% (4 units/mL)<sup>14</sup> in phosphate buffered saline (PBS). Trypsin inhibitors aprotinin and leupeptin (Sigma–Aldrich) were added to the PLC solution at concentrations of 5 µg/mL<sup>14</sup>.

### Tissue acquisition

Osteochondral plugs were harvested from 1–3 week old bovine joints as previously described<sup>19,20</sup> from locations M1 and M4 of the distal femoral condyles, corresponding to medial anterior and medial posterior locations, respectively. These locations were selected for comparison of regions subjected to relatively high and low contact pressure<sup>19</sup>, and hereafter will be referred to as M1 and M4, respectively. Plugs were stored at 37°C and 5% CO<sub>2</sub> in culture

medium<sup>20</sup> for 24 h, and trimmed to 1.5 mm in height with a custom cutting jig and razor prior to AFM measurements.

### Friction coefficient and surface roughness

Nanoscale friction and surface roughness measurements were acquired with an AFM (MFP-3D-CF, Asylum Research, Santa Barbara, CA) with triangular silicon nitride (Si<sub>3</sub>N<sub>4</sub>) tips (MSCT-AUNM, Veeco Instruments, Santa Barbara, CA) of 10 nm nominal radius and 0.01 N/m spring constant. Surface scanning of 60 × 60 µm<sup>2</sup> areas was performed in contact mode using the parameters: matrix size = 128 × 128 pixels, scan frequency = 1 Hz, and set point = 2.5 V, which corresponded to a load of 2.13 ± 0.04 nN, determined by thermal calibration<sup>21</sup> performed on glass. Lateral force calibration performed on silicon grating (TGF11, Mikromasch, Wilsonville, OR) using the direct force balance method<sup>22</sup> showed that the friction voltage and friction force were related by a constant of 102.64 nN/V. The friction coefficient  $\mu$  was obtained as the ratio of the measured friction force to the applied normal load.

Samples ( $n=6$ ) were affixed with ethyl cyanoacrylate to a custom sample holder with the articular surface facing upward. Each control sample was first treated with 20 µL of PBS and scanned at five different locations while immersed in PBS. Subsequently, the surface was treated with 20 µL of the respective enzyme for 15 min (trypsin or hyaluronidase)<sup>15</sup> or 1 h (PLC)<sup>14</sup> and rinsed in PBS. Treated samples were scanned at five different locations in PBS. The average friction force was determined as half of the difference between the mean lateral trace and retrace values<sup>12,23</sup>. Surface roughness  $R_s$  was measured as the root-mean-square (RMS) deviation from the average surface height at five locations per sample.

### Adhesion and stiffness

Because trypsin had the most significant effect on articular cartilage friction (see Results), further experiments were performed to investigate the friction mechanisms in the boundary lubrication regime. Adhesion and stiffness of control and trypsin-digested cartilage surfaces ( $n=4$ ) were studied with an AFM. Five force–displacement curves were obtained from five different locations of each sample surface (i.e., 25 per sample) using the parameters: set point = 3 V (2.56 nN), trigger point = 6 V (5.12 nN), load/unload speed = 2 µm/s, and dwell time = 0.99 s. The tip displacement  $\delta$  was calculated as the difference between the  $z$ -position of the piezoelectric transducer and the measured deflection of the cantilever tip  $d$ , i.e.,  $\delta = z - d$ .

Stiffness was determined from the slope of the force–displacement response at the onset of unloading from the maximum tip displacement<sup>11,24,25</sup>. Adhesion force was measured as the pull-off force upon tip separation from the surface during unloading. Adhesion hysteresis was calculated as the area enclosed by the loading and unloading paths of the force–displacement response<sup>26</sup>.

### Guanidine extraction and quantification of surface SZP

SZP concentration (µg/mL) at the surface of treated and untreated samples ( $n=3$ ) was quantified by enzyme-linked immunosorbant assay (ELISA). Surfaces were treated with trypsin as described above, and SZP was extracted from the surface for 15 min at room temperature, using 20 µL of 4 M guanidine-HCl with 0.05 M Tris, 1 mM protease inhibitor cocktail (PIC), and 1 mM phenylmethanesulphonyl fluoride (PMSF). The extracts were buffer exchanged with 6 M urea containing 0.05 M Tris<sup>19</sup>. Serially diluted samples of the extracts were reacted with S6.79 (1:5000) (a generous gift from Tom Schmid, Rush Medical University) as the

primary antibody<sup>19</sup> and anti-mouse horseradish peroxidase-conjugated goat (1:3000, Vector Laboratories, Burlingame, CA) as the secondary antibody.

#### Immunohistochemistry (IHC)

Immunolocalization of SZP by IHC was performed on trypsin-treated samples ( $n = 3$ ), the group that showed significant differences in  $\mu$  following enzymatic digestion. Samples were treated as described above and fixed in Bouin's solution overnight, followed by paraffin embedding and sectioning. Immunostaining was performed using S6.79 (1:5000) as the primary antibody and an ABC kit (Vector Laboratories) with mouse IgG as secondary antibody. Images were obtained with an optical microscope (LSM 510, Carl Zeiss, Jena, Germany) at 100 $\times$  magnification.

To determine if other surface structures were affected by trypsin, additional stains were applied to separate sections. Staining was accomplished using hematoxylin (Vector Laboratories) for 7 min, light green SF yellowish (L-1886, Sigma–Aldrich) for 5 min, and safranin O (JT Baker, Pittsburgh, PA) for 5 min. Images were obtained with an optical microscope at 20 $\times$  and 40 $\times$  magnifications.

#### Transmission electron microscopy

Structural changes at the surface of trypsin-treated samples were examined with a transmission electron microscope (TEM). Untreated and trypsin-treated plugs ( $n = 1$ ) were fixed in Karnovsky's fixative (Electron Microscopy Sciences, Hatfield, PA) overnight at 4°C. A drop of liquefied 2% agarose was added to stabilize the pellet. Samples were placed in 1% osmium tetroxide in 0.1 M phosphate buffer for 1 h on ice, and then in 1% tannic acid in water for 30 min on ice. Samples were stained *en bloc* with 2% uranyl acetate for 1 h on ice and dehydrated in a series of increasing concentrations of acetone (30–100%, 10 min each grade). Samples were embedded in a 50:50 acetone:bojax (epon/araldite) mixture overnight at room temperature, transferred into 100% resin for 2 h, then transferred into fresh resin and polymerized at 70°C overnight. Sections were cut with a diamond knife and stained with uranyl acetate and lead citrate before viewing with a Philips 120 BioTwin microscope (FEI, Lausanne, Switzerland) at 80 kV. Images were acquired at 6500 $\times$  and 15,000 $\times$  magnifications.

#### Statistical analysis

Differences in average  $\mu$  and  $R_s$  were analyzed ( $n = 6$ ) using a one-way nested analysis of variance (ANOVA) with four treatment levels (M1 control, M1 treatment, and M4 control, M4 treatment as fixed effects) and sample number and measurement number (five locations) as subgroups, per enzyme group. Differences in average adhesion force, adhesion hysteresis, and stiffness between control and trypsin-treated samples were analyzed ( $n = 4$ ) using a one-way nested ANOVA with four treatment levels and sample number and measurement number (25 force curves) as subgroups. A nested analysis was used to account for multiple measurements and explant animals for each treatment. A significance level of  $\alpha = 0.05$ , and corresponding  $P < 0.0083$ , was used to determine differences between groups in all the tests. Results are presented as mean  $\pm 1.96 \times$  standard error of the mean (S.E.M.).

## Results

#### Friction coefficient and surface roughness

All enzyme treatments showed a general trend of higher friction compared to both M1 and M4 controls (Fig. 1). Trypsin increased  $\mu$

of both M1 and M4 samples most significantly ( $\mu_{\text{ctrl}} = 0.23 \pm 0.03$  vs  $\mu_{\text{treat}} = 0.52 \pm 0.08$  for M1 ( $P < 0.0001$ ) and  $\mu_{\text{ctrl}} = 0.24 \pm 0.04$  vs  $\mu_{\text{treat}} = 0.46 \pm 0.09$  for M4 ( $P < 0.0001$ )) [Fig. 1(A)]. M1 samples also showed a significant increase in  $\mu$  after PLC treatment ( $\mu_{\text{ctrl}} = 0.31 \pm 0.05$  vs  $\mu_{\text{treat}} = 0.49 \pm 0.08$  ( $P = 0.0145$ )) [Fig. 1(C)]. All other groups did not show significant differences.

Surface roughness did not demonstrate a consistent trend or significant change for any enzyme treatment or joint location [Fig. 2 (A–C)]. Topography images did not reveal any discernible differences between control and corresponding treated M1 and M4 samples for all enzymes [Fig. 2(D–E); images of PLC group not shown for brevity]. Fibrillated and amorphous surface structures were observed in the AFM images, in agreement with reports of previous studies<sup>20,23</sup>. Images shown in Fig. 2(D–E) correspond to a sample group (trypsin or hyaluronidase) of surface roughness within the range of the average RMS roughness of all samples measured.

#### Adhesion and stiffness

Friction results led to additional assays on trypsin-treated cartilage surfaces to determine the role of SZP/proteins in friction. Figure 3(A) shows a schematic of the force–distance response. After trypsin treatment, the contact stiffness of M1 samples decreased significantly from  $28.63 \pm 0.10$  to  $16.53 \pm 0.09$  mN/m ( $P < 0.0001$ ), whereas that of M4 samples increased significantly from  $15.76 \pm 0.10$  to  $24.62 \pm 0.22$  mN/m ( $P < 0.0001$ ) [Fig. 3(B)]. M1 controls exhibited significantly higher stiffness compared to M4 controls ( $P < 0.0001$ ).

Adhesion force (0.04–1.22 nN) exceeded 50% of the applied load (2.13 nN) in some cases. Undigested M1 controls also demonstrated significantly higher adhesion forces than M4 controls ( $P < 0.0001$ ), and trypsin treatment resulted in significantly lower adhesion forces for both M1 ( $P < 0.0001$ ) and M4 ( $P < 0.0005$ ) [Fig. 3(C)]. Differences in adhesion between trypsin-treated M1 and M4 samples were insignificant. Adhesion force of M1 and M4 samples decreased from  $1.22 \pm 0.11$  to  $0.04 \pm 0.01$  nN and from  $0.24 \pm 0.04$  to  $0.16 \pm 0.02$  nN, respectively. An adhesion hysteresis, demonstrating a pattern similar to that of the adhesion force, was also observed [Fig. 3(E–H)]. Adhesion hysteresis of M1 and M4 samples decreased from  $0.68 \pm 0.07$  to  $0.01 \pm 0.004$  nN  $\mu\text{m}$  ( $P < 0.0001$ ) and from  $0.08 \pm 0.02$  to  $0.06 \pm 0.015$  nN  $\mu\text{m}$  ( $P < 0.0001$ ), respectively [Fig. 3(D)].

#### Quantification and visualization of SZP at the surface

SZP was removed from the cartilage surface following trypsin treatment. SZP decreased dramatically at the surface of both M1 and M4 samples after trypsin digestion ( $P = 0.005$ ) [Fig. 4(A)]. The surface concentration of SZP in M1 and M4 controls was  $1.62 \pm 0.38$   $\mu\text{g}/\text{mL}$  ( $0.0016 \pm 0.0004$   $\mu\text{g}/\text{mm}^2$ , normalized to the cross-section area) and  $0.89 \pm 0.12$   $\mu\text{g}/\text{mL}$  ( $0.0009 \pm 0.0001$   $\mu\text{g}/\text{mm}^2$ ), respectively. After digestion, SZP surface concentration decreased below the detection limit of the ELISA system (0.0625  $\mu\text{g}/\text{mL}$ ) and was considered to be negligible.

IHC showed a dramatic decrease in depth of staining of SZP for both M1 and M4 trypsin-treated samples compared to controls [Fig. 4(B)]. TEM revealed that trypsin disrupted the lamina splendens reported in previous studies<sup>27–29</sup>, removing most or all of the cloudy amorphous structures (blue arrows) present in the untreated samples [Fig. 4(C)]. These structures differ from collagen fibers (green arrowheads) and may be the proteoglycan content that provides boundary lubrication of articular cartilage.

Safranin O and light green staining showed a slight decrease in proteoglycan content after trypsin treatment for both M1 and M4

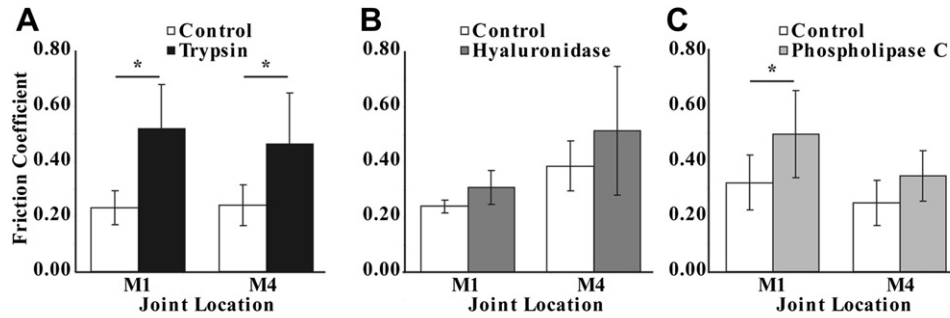


**Fig. 1.** The friction coefficient of articular surfaces measured with an AFM ( $n = 6$ ) increased significantly after trypsin treatment for both M1 and M4 locations (A), while hyaluronidase treatment did not result in significant changes in friction coefficient (B) and PLC treatment caused a significant increase in friction coefficient only for cartilage from M1 joint location (C). Error bars indicate  $1.96 \times$  s.e.m. above and below corresponding mean values. Significant differences in the data of each group are indicated by an asterisk ( $P \leq 0.0145$ ).

(Fig. 5). Loss of proteoglycans was most distinct in the superficial zone. Collagen content did not markedly change after trypsin treatment in either location.

### Discussion

This study sought to elucidate the roles of SZP, HA, and SAPL in boundary lubrication of articular cartilage and determine the dominant friction mechanism through systematic removal of candidate molecules *in situ*. Results showed that (1) trypsin significantly increased  $\mu$  of cartilage from both load-bearing (M1) and non load-bearing (M4) locations (Fig. 1) (2)  $R_s$  did not change significantly after enzyme digestion [Fig. 2(A–C)] and did not correspond to  $\mu$  changes (3) SZP was eliminated from the surface

after trypsin treatment [Fig. 4(A–B)] (4) adhesion force and adhesion hysteresis of M1 and M4 samples decreased significantly after trypsin treatment [Fig. 3(C–D)]; and (5) proteoglycans in M1 and M4 samples decreased after trypsin treatment (Fig. 5). These findings suggest that the proteinaceous component of the articular cartilage surface contributes most to boundary lubrication of the tissue and that the effects of roughness and adhesion on friction are secondary.

The increase in  $\mu$  after trypsin digestion indicates a loss of the boundary lubricant, with SZP as the strongest candidate. The role of SZP as a key boundary lubricant of articular cartilage is suggested by its large central mucin domain<sup>3,5</sup> and localized expression at synovial joint surfaces<sup>30,31</sup>. Furthermore, most of the SZP produced in the joint is secreted from the tissue into the synovial fluid rather

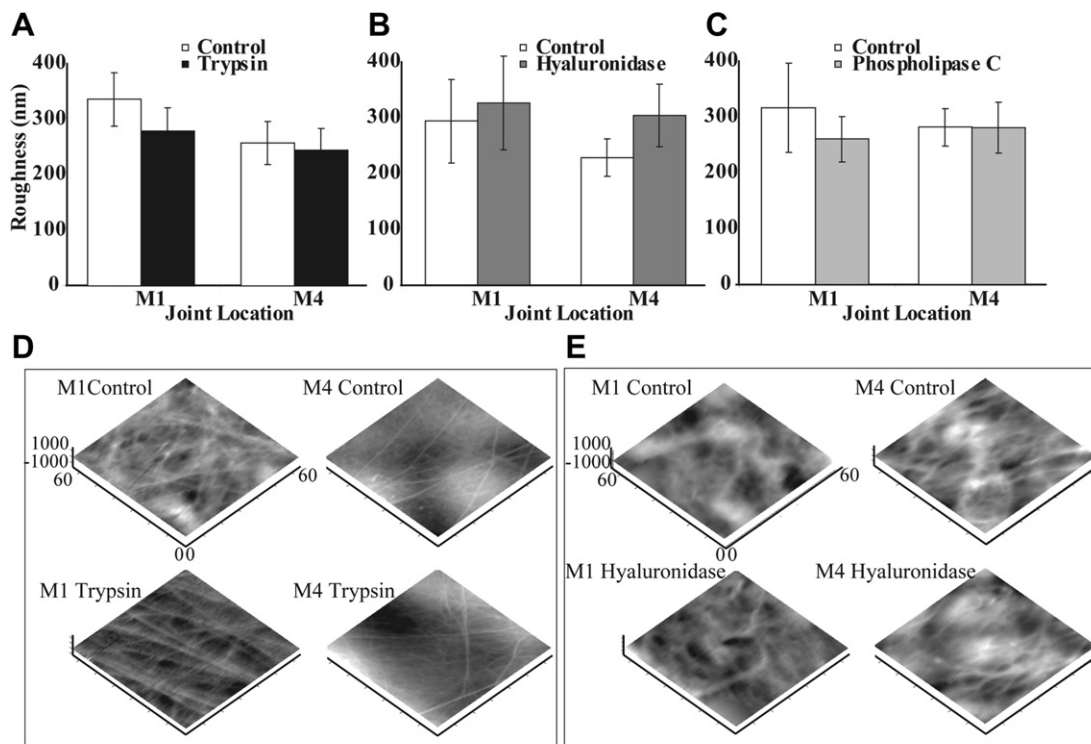


**Fig. 2.** The RMS surface roughness of articular cartilage surfaces ( $n = 6$ ) did not change significantly after treatment with (A) trypsin, (B) hyaluronidase, and (C) PLC. Representative AFM topography images of articular cartilage surfaces treated with (D) trypsin and (E) hyaluronidase revealed the fibrillar and amorphous structures of the cartilage surface. The topographies of samples treated with PLC (not shown) generally appeared similar to those treated with hyaluronidase. Error bars in (A–C) indicate  $1.96 \times$  s.e.m. above and below corresponding mean values.

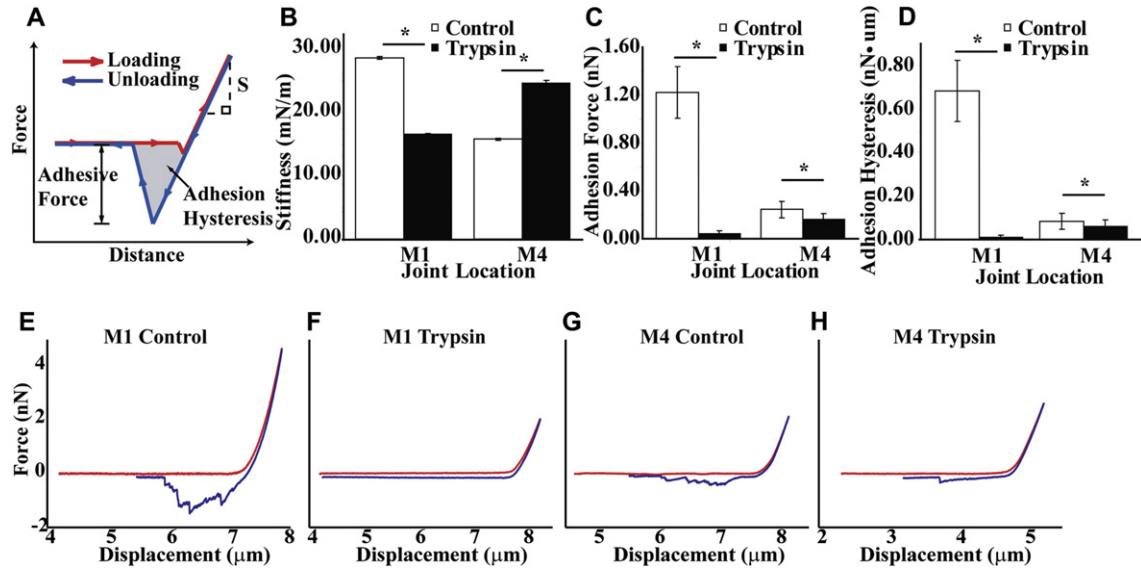


**Fig. 3.** (A) Schematic of force–distance response obtained with an AFM. Contact stiffness was determined from the slope *S* of the unloading path at the maximum tip displacement. Adhesion force was measured as the pull-off force at the instant the AFM tip separated from the sample surface. Adhesion hysteresis was calculated as the area enclosed by the loading and the unloading paths of the force–distance response. (B) The contact stiffness changed differently after trypsin digestion depending on sample harvest location, indicative of the differences in molecular constituents and enzymatic susceptibility between joint regions of high and low contact pressure. (C, D) Adhesion force and adhesion hysteresis decreased significantly in both M1 and M4 joint regions after trypsin treatment (*n* = 4). (E, H) Representative force–displacement curves for control and trypsin-treated cartilage surfaces. Error bars in (B–D) indicate  $1.96 \times$  s.e.m. above and below corresponding mean values. Significantly different values are denoted by an asterisk ( $P \leq 0.0005$ ).

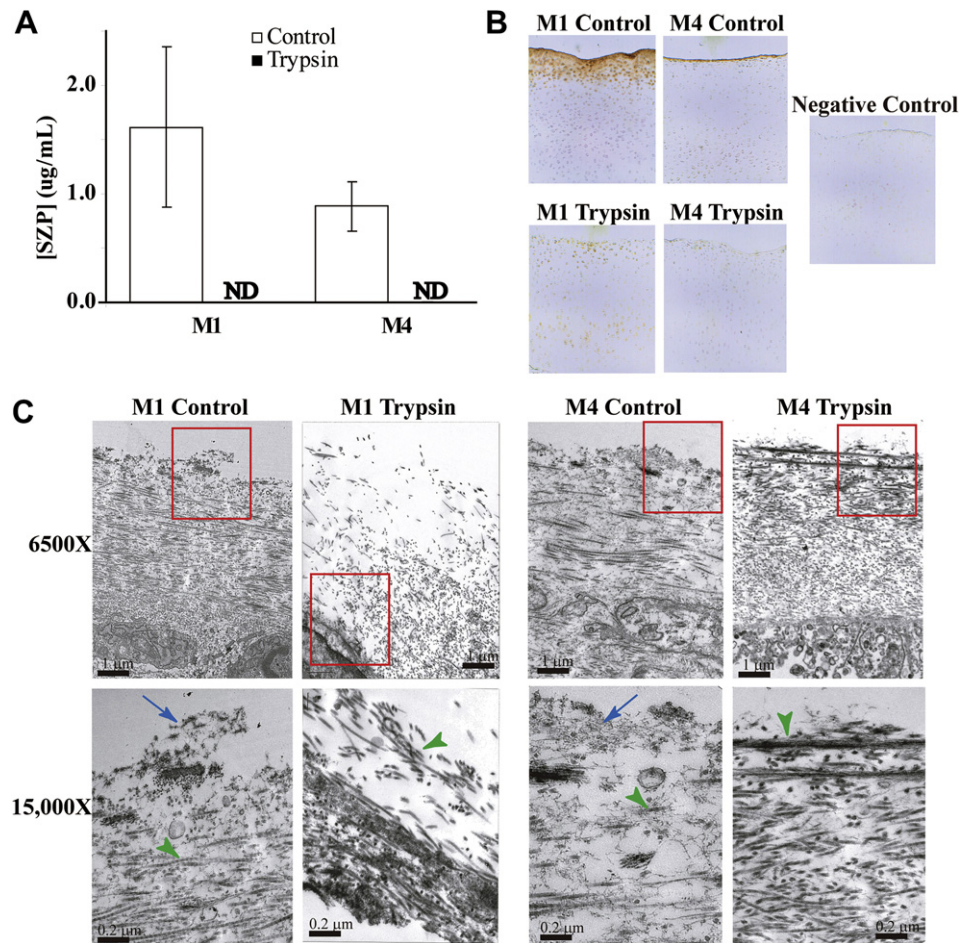


**Fig. 4.** (A) Concentration of SZP at the surface of articular cartilage after trypsin digestion (ND = not detectable) (*n* = 3). Error bars indicate  $1.96 \times$  s.e.m. above and below corresponding mean values. (B) IHC showing differences in SZP distribution in control and trypsin-treated cartilage surfaces. (C) TEM images showing the surface structure in control and trypsin-treated articular cartilage (bottom row shows high-magnification images of the regions enclosed by a rectangle in the images of the row above).

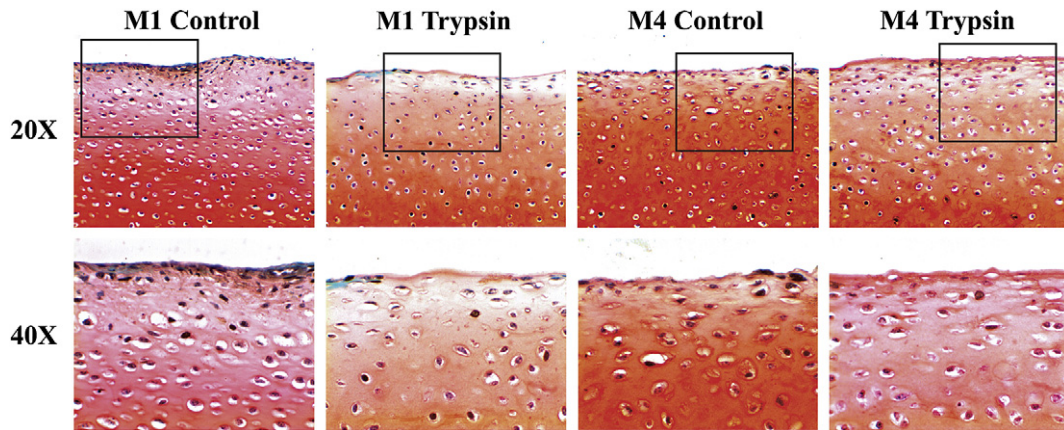


**Fig. 5.** The proteoglycan content stained with safranin O (red) decreased after trypsin treatment, particularly in the uppermost layer of the superficial zone. The collagen content stained with light green (blue–green) showed no dramatic changes after trypsin treatment. Bottom row shows high-magnification images of the regions enclosed by a rectangle in the images of the row above.

than retained within the matrix<sup>30</sup>, suggesting a critical function at the articular surface. SZP has also been found to localize in the synovial lining of joint cavities<sup>31</sup>, meniscus<sup>32</sup>, and tendon<sup>33</sup>, providing further evidence of a surface-interacting molecule. Mutations in the *PRG4* gene that encodes SZP have also been associated with the joint disease camptodactyly–arthopathy–coxa vara–pericarditis, which may cause premature joint wear as a consequence of insufficient lubrication<sup>3,4</sup>. Cartilage of *PRG4*-deficient mice have also been shown to exhibit higher friction coefficients than wild type<sup>34,35</sup>. Together with the results of the present investigation, the evidence strongly supports SZP as the key boundary lubricant of articular cartilage.

The observed friction behavior was attributed to a plowing mechanism. Friction coefficient changes did not correspond to surface roughness changes, consistent with previous reports<sup>10</sup>; however adhesion decreased significantly after trypsin digestion. In general, friction is due to asperity deformation (roughness effect), adhesion (surface energy effect), and plowing by asperities and wear particles (material deformation effect)<sup>10,12</sup>. Adhesion force and hysteresis typically scale proportionally with friction force<sup>36</sup>, although an inverse or nonexistent relationship has been shown for various material coatings and that other mechanisms may dominate the friction behavior<sup>37,38</sup>. Therefore, it is likely that the dominant friction mechanism of articular cartilage, studied at the nanoscale in buffer solution, is not adhesion. Since the contributions of surface roughness and adhesion to friction were found to be secondary, the observed friction behavior may be due to a dominant plowing mechanism. Because  $\text{Si}_3\text{N}_4$  is much harder than cartilage, it may be inferred that plowing of the cartilage surface by the AFM tip prevailed under the applied contact pressure ( $\sim 1.5$  MPa), resulting in energy dissipation in the form of irreversible deformation and wear. In view of the viscoelastic behavior of articular cartilage, energy could have also been dissipated in the form of elastic hysteresis. The plowing mechanism may also explain the increase in  $\mu$  after trypsin treatment if enzymatic digestion produced cleaved but still adsorbed fragments of proteins at the surface. Additional testing showed an increase in friction coefficient dependence on sliding speed<sup>39</sup>, and indicated a dominant effect from plowing (Fig. S1).

Trypsin is a wide-spectrum protease that degrades proteins at the carboxy-terminal domains in lysine and arginine residues. SZP contains an abundance of both, especially lysine found at the start of each repeat sequence in the mucin region<sup>5</sup>. This lubricating region of SZP would therefore be hydrolyzed extensively by trypsin,

as verified in this study [Fig. 4(A–B)] and previously<sup>13</sup>. Digestion by trypsin would also affect other proteins at the surface, such as albumin, fibronectin, and aggrecan<sup>40</sup>. Sliding of non-functionalized AFM tips against aggrecan monolayers yielded higher friction compared to tips with end-grafted aggrecan and also an increase in friction with decreasing GAG spacing<sup>41</sup>, demonstrating that a decrease in aggrecan and other proteoglycan content at the articular surface leads to increased friction. Furthermore, because SZP binds to some of these proteins, there is an additive effect of trypsin to the boundary lubricating properties of articular cartilage. While SZP is the most likely proteinaceous boundary lubricant with the strongest evidence of lubricating efficacy, digestion of other surface proteins and SZP-binding proteins may affect  $\mu$ . HA binds to SZP<sup>40</sup> and, although not directly digested by trypsin, it may be dissociated from the surface after digestion of SZP or aggrecan. However, direct digestion of HA by hyaluronidase did not increase  $\mu$  significantly [Fig. 1(B)].

Hyaluronidase specifically hydrolyzes the endo-N-acetyl-D-glucosamine bonds in HA, which does not affect SZP lubricity<sup>3</sup>. Results showed that HA did not significantly change  $\mu$  after enzymatic removal [Fig. 1(B)], consistent with previous findings showing inferior boundary lubrication by HA and its derivatives compared to synovial fluid, isolated lubricin<sup>6,42</sup>, and intact articular cartilage<sup>43</sup>. Thus HA likely does not provide boundary lubrication in the absence of other surface-interacting molecules. Additional assays of hyaluronidase efficacy using biotinylated HA-binding protein (b-HABP)<sup>13</sup> showed that HA content at the surface was reduced by enzyme treatment compared to controls at both joint locations (Fig. S2). Since it appeared that complete removal of HA was not achieved, with surfaces stained lightly for b-HABP after enzyme treatment, longer incubation (2–43 h)<sup>13,15,18</sup> may have resulted in complete removal of HA, but would likely have not increased friction significantly, as demonstrated by others<sup>13,18</sup>. Isolated HA and SZP have been reported to produce similar low  $\mu$  when tested individually in a cartilage–cartilage system, with  $\mu$  approaching that of synovial fluid<sup>8</sup> when HA and SZP were combined. However, the previous studies examined the effects of synovial fluid constituents on friction in a cartilage–cartilage sliding system, while the present study examined the effects of removing surface molecules from cartilage using an AFM. HA is found in high concentrations in synovial fluid<sup>44</sup> and much lower concentrations in the lamina splendens and superficial zone<sup>28</sup> of cartilage and the role of HA in cartilage tissue may not be as important in joint lubrication as in synovial fluid. A similar

enhancement of lubrication was observed when combinations of HA and SZP were incorporated in synovial fluid<sup>45</sup>, although their synergistic effects on articular cartilage were not reported. Future studies should focus on the combined effects of all three putative boundary lubricants.

Addition of trypsin inhibitors to PLC ensured the specific degradation of SAPL without proteolysis. Results showed a minor effect of SAPL digestion on  $\mu$  [Fig. 1(C)], consistent with previous results demonstrating the lubricity of synovial fluid digested with PLC<sup>14</sup>. An intermediate effect of PLC on tendon friction (between that of hyaluronidase and trypsin) has also been reported<sup>13</sup>. Addition of SAPL alone or in conjunction with HA and SZP does not reduce  $\mu$  significantly<sup>8</sup>. Although SAPL may impart hydrophobic surface characteristics, this alone cannot explain the excellent lubrication properties of articular cartilage. Decreased hydrophobicity had a significant effect on  $\mu$  of M1 but not M4 samples [Fig. 1(C)], indicating a relatively minor role of SAPL in articular cartilage boundary lubrication.

Differences between M1 and M4 samples in the PLC group indicate a dependence of molecular composition, enzymatic susceptibility, and nanomechanical properties of articular cartilage on anatomical location. SZP distribution depends on both the zone within the thickness of the tissue and the anatomical regions of the joint<sup>19,46</sup>. Similar zonal and regional dependence of GAG and proteoglycan contents and their different metabolism rates in different joint regions have been observed<sup>19,47,48</sup>. Load-bearing locations contain more GAG and proteoglycan than non load-bearing locations. Cartilage from load-bearing locations is also more susceptible to early proteoglycan synthesis inhibition and increased expression of catabolic cytokines caused by osteoarthritis<sup>48</sup>. Higher collagen type I and II gene expressions have also been found in load-bearing than non load-bearing regions<sup>49</sup>; however, protein expression was not measured. Although SAPL distribution across different joint locations has not been investigated, it is reasonable to assume that it varies in a manner similar to other important cartilage components according to functional loading. The stiffness response of M1 and M4 samples to trypsin treatment [Fig. 3(B)] may also be explained by these differences. Higher initial GAG, proteoglycan, and collagen contents in M1 control samples would impart higher mechanical strength at the surface compared to M4. Indeed, a higher compressive stiffness was found for M1 compared to M4 controls [Fig. 3(B)]. After trypsin treatment, M1 stiffness decreased to that of undigested M4 samples, which would be expected after the removal of proteoglycans, as evidenced from histology results (Fig. 5). Cartilage surfaces of similar low stiffness cartilage and low GAG staining have been reported for PRG4-knockout mice<sup>34,35</sup>. The stiffness increase of M4 samples after trypsin treatment is unexpected and may be associated with differences in molecular composition and chemical/mechanical responses to enzymatic degradation between load-bearing and non load-bearing regions. Any changes in the surface mechanical strength would likely also affect friction, because of the interdependence of material properties and friction mechanisms<sup>50</sup>. The increase in nanoscale stiffness with decreasing GAGs reported in previous studies<sup>11,25</sup>, has been attributed to tissue dehydration due to loss of electrostatic repulsive forces and subsequently the AFM measuring the stiffness of the underlying collagen network rather than the normally proteoglycan-covered surface<sup>11</sup>. As was verified by TEM images, the collagen network was indeed exposed in trypsin-treated M4 samples; therefore the stiffness measured with the AFM was that of collagen and not that of the decreased GAG containing surface.

The proteinaceous content of the articular cartilage surface exhibited the most significant effect on friction. SZP plays a critical role in the boundary lubrication of articular cartilage. Loss of SZP by

trypsin surface treatment increased  $\mu$  in both load-bearing and non load-bearing regions. Although HA and SAPL may enhance SZP function, the results of this study demonstrate that they play relatively secondary roles in reducing friction and protecting the joint against wear.

#### Conflict of interest

The authors have no conflicts of interest to disclose.

#### Supplementary material

Supplementary material for this article is available in the online version at [doi:10.1016/j.joca.2010.03.012](https://doi.org/10.1016/j.joca.2010.03.012).

#### References

- Mow VC, Ratcliffe A, Poole AR. Cartilage and diarthrodial joints as paradigms for hierarchical materials and structures. *Biomaterials* 1992;13:67–97.
- Hills BA. Boundary lubrication in vivo. *Proc Inst Mech Eng H* 2000;214:83–94.
- Jay GD, Harris DA, Cha CJ. Boundary lubrication by lubricin is mediated by O-linked beta(1-3)Gal-GalNAc oligosaccharides. *Glycoconj J* 2001;18:807–15.
- Marcelino J, Carpten JD, Suwairi WM, Gutierrez OM, Schwartz S, Robbins C, et al. CACP, encoding a secreted proteoglycan, is mutated in camptodactyly-arthropathy-coxa vara-pericarditis syndrome. *Nat Genet* 1999;23:319–22.
- Flannery CR, Hughes CE, Schumacher BL, Tudor D, Aydelotte MB, Kuettner KE, et al. Articular cartilage superficial zone protein (SZP) is homologous to megakaryocyte stimulating factor precursor and is a multifunctional proteoglycan with potential growth-promoting, cytoprotective, and lubricating properties in cartilage metabolism. *Biochem Biophys Res Commun* 1999;254:535–41.
- Benz M, Chen N, Israelachvili J. Lubrication and wear properties of grafted polyelectrolytes, hyaluronan and hylan, measured in the surface forces apparatus. *J Biomed Mater Res A* 2004;71:6–15.
- Marshall KW. Intra-articular hyaluronan therapy. *Curr Opin Rheumatol* 2000;12:468–74.
- Schmidt TA, Gastelum NS, Nguyen QT, Schumacher BL, Sah RL. Boundary lubrication of articular cartilage: role of synovial fluid constituents. *Arthritis Rheum* 2007;56:882–91.
- Schwarz IM, Hills BA. Surface-active phospholipid as the lubricating component of lubricin. *Br J Rheumatol* 1998;37:21–6.
- Coles JM, Blum JJ, Jay GD, Darling EM, Guilak F, Zauscher S. In situ friction measurement on murine cartilage by atomic force microscopy. *J Biomech* 2008;41:541–8.
- Stolz M, Gottardi R, Raiteri R, Miot S, Martin I, Imer R, et al. Early detection of aging cartilage and osteoarthritis in mice and patient samples using atomic force microscopy. *Nat Nanotechnol* 2009;4:186–92.
- Bhushan B. *Handbook of Micro/Nanotribology*. 2nd edn. Boca Raton, LA: CRC Press; 1999.
- Sun Y, Chen MY, Zhao C, An KN, Amadio PC. The effect of hyaluronidase, phospholipase, lipid solvent and trypsin on the lubrication of canine flexor digitorum profundus tendon. *J Orthop Res* 2008;26:1225–9.
- Jay GD, Cha CJ. The effect of phospholipase digestion upon the boundary lubricating ability of synovial fluid. *J Rheumatol* 1999;26:2454–7.
- Wilkins J. Proteolytic destruction of synovial boundary lubrication. *Nature* 1968;219:1050–1.

16. Hills BA, Monds MK. Enzymatic identification of the load-bearing boundary lubricant in the joint. *Br J Rheumatol* 1998;37:137–42.
17. Kumar P, Oka M, Toguchida J, Kobayashi M, Uchida E, Nakamura T, et al. Role of uppermost superficial surface layer of articular cartilage in the lubrication mechanism of joints. *J Anat* 2001;199:241–50.
18. Roberts BJ, Unsworth A, Mian N. Modes of lubrication in human hip joints. *Ann Rheum Dis* 1982;41:217–24.
19. Neu CP, Khalafi A, Komvopoulos K, Schmid TM, Reddi AH. Mechanotransduction of bovine articular cartilage superficial zone protein by transforming growth factor  $\beta$  signaling. *Arthritis Rheum* 2007;56:3706–14.
20. DuRaine G, Neu CP, Chan SM, Komvopoulos K, June RK, Reddi AH. Regulation of the friction coefficient of articular cartilage by TGF- $\beta$ 1 and IL-1 $\beta$ . *J Orthop Res* 2009;27:249–56.
21. Hutter J, Bechhoefer J. Calibration of atomic force microscope tips. *Rev Sci Instrum* 1993;64:1868–73.
22. Asay DB, Kim SH. Direct force balance method for atomic force microscopy lateral force calibration. *Rev Sci Instrum* 2006;77:1–9.
23. Park S, Costa KD, Ateshian GA. Microscale frictional response of bovine articular cartilage from atomic force microscopy. *J Biomech* 2004;37:1679–87.
24. Oliver WC, Pharr GM. An improved technique for determining hardness and elastic modulus using load and displacement sensing indentation experiments. *J Mater Res* 1992;7:1564–83.
25. Stolz M, Raiteri R, Daniels AU, VanLandingham MR, Baschong W, Aebi U. Dynamic elastic modulus of porcine articular cartilage determined at two different levels of tissue organization by indentation-type atomic force microscopy. *Biophys J* 2004;86:3269–83.
26. Gavaille J, Takadoum J. Surface charges and adhesion measured by atomic force microscope influence on friction. *Tribol Int* 2003;36:865–71.
27. Bhatnagar R, Christian RG, Nakano T, Aherne FX, Thompson JR. Age related changes and osteochondrosis in swine articular and epiphyseal cartilage: light and electron microscopy. *Can J Comp Med* 1981;45:188–95.
28. Orford CR, Gardner DL. Ultrastructural histochemistry of the surface lamina of normal articular cartilage. *Hist J* 1985;17:223–33.
29. Jay GD, Torres JR, Rhee DK, Helminen HJ, Hytinen MM, Cha CJ, et al. Association between friction and wear in diarthrodial joints lacking lubricin. *Arthritis Rheum* 2007;56:3662–9.
30. Schumacher BL, Block JA, Schmid TM, Aydelotte MB, Kuettner KE. A novel proteoglycan synthesized and secreted by chondrocytes of the superficial zone of articular cartilage. *Arch Biochem Biophys* 1994;311:144–52.
31. Schumacher BL, Hughes CE, Kuettner KE, Caterson B, Aydelotte MB. Immunodetection and partial cDNA sequence of the proteoglycan, superficial zone protein, synthesized by cells lining synovial joints. *J Orthop Res* 1999;17:110–20.
32. Schumacher BL, Schmidt TA, Voegtline MS, Chen AC, Sah RL. Proteoglycan 4 (PRG4) synthesis and immunolocalization in bovine meniscus. *J Orthop Res* 2005;23:562–8.
33. Rees SG, Davies JR, Tudor D, Flannery CR, Hughes CE, Dent CM, et al. Immunolocalisation and expression of proteoglycan 4 (cartilage superficial zone proteoglycan) in tendon. *Matrix Biol* 2002;21:593–602.
34. Coles JM, Cha J, Warman ML, Jay GD, Guilak F, Zauscher S. Frictional, mechanical, and morphological differences between PRG4 (+/+) and (-/-) mice measured by atomic force microscopy. In: 53rd Annual Meeting of the Orthopaedic Research Society. San Diego, CA 2007.
35. Coles JM, Cha J, Blum JJ, Cheng AC, Warman ML, Jay GD, et al. Microscale surface properties of PRG4 knockout joints measured as a function of age. In: 55th Annual Meeting of the Orthopaedic Research Society. San Francisco, CA 2009.
36. Israelachvili J, Chen Y, Yoshizawa H. Relationship between adhesion and friction forces. *J Adhes Sci Technol* 1994;8:1231–49.
37. Carpick RW, Flater EE, Sridharan K. The effect of surface chemistry and structure on nano-scale adhesion and friction. *Polym Mater Sci Eng* 2004;90:197–8.
38. Liu H, Bhushan B, Eck W, Stadler V. Investigation of the adhesion, friction, and wear properties of biphenyl thiol self-assembled monolayers by atomic force microscopy. *J Vac Sci Technol A* 2001;19:1234–40.
39. Rennie AC, Dickrell PL, Sawyer WG. Friction coefficient of soft contact lenses: measurements and modeling. *Tribol Lett* 2005;18:499–504.
40. Schmid T, Homandberg G, Madsen L, Su J, Kuettner K. Superficial zone protein (SZP) binds to macromolecules in the lamina splendens of articular cartilage. In: 48th Annual Meeting of the Orthopaedic Research Society. Dallas, TX 2002.
41. Han L, Dean D, Mao P, Ortiz C, Grodzinsky AJ. Nanoscale shear deformation mechanisms of opposing cartilage aggrecan macromolecules. *Biophys J* 2007;93:L23–5.
42. Jay GD, Haberstroh K, Cha CJ. Comparison of the boundary-lubricating ability of bovine synovial fluid, lubricin, and Healon. *J Biomed Mater Res* 1998;40:414–8.
43. Kawai N, Tanaka E, Takata T, Miyauchi M, Tanaka M, Todoh M, et al. Influence of additive hyaluronic acid on the lubricating ability in the temporomandibular joint. *J Biomed Mat Res A* 2004;70:149–53.
44. Decker B, Mc GW, Mc KB, Slocumb CH. Concentration of hyaluronic acid in synovial fluid. *Clin Chem* 1959;5:465–9.
45. Jay GD, Lane BP, Sokoloff L. Characterization of a bovine synovial fluid lubricating factor. III. The interaction with hyaluronic acid. *Connect Tissue Res* 1992;28:245–55.
46. Young AA, McLennan S, Smith MM, Smith SM, Cake MA, Read RA, et al. Proteoglycan 4 downregulation in a sheep meniscectomy model of early osteoarthritis. *Arthritis Res Ther* 2006;8:R41.
47. Rogers BA, Murphy CL, Cannon SR, Briggs TW. Topographical variation in glycosaminoglycan content in human articular cartilage. *J Bone Joint Surg Br* 2006;88:1670–4.
48. Dumond H, Presle N, Pottier P, Pacquelet S, Terlain B, Netter P, et al. Site specific changes in gene expression and cartilage metabolism during early experimental osteoarthritis. *Osteoarthritis Cartilage* 2004;12:284–95.
49. Lorenz H, Wenz W, Ivancic M, Steck E, Richter W. Early and stable upregulation of collagen type II, collagen type I and YKL40 expression levels in cartilage during early experimental osteoarthritis occurs independent of joint location and histological grading. *Arthritis Res Ther* 2005;7:R156–65.
50. Dean D, Han L, Grodzinsky AJ, Ortiz C. Compressive nano-mechanics of opposing aggrecan macromolecules. *J Biomech* 2006;39:2555–65.